Arl13b regulates ciliogenesis and the dynamic localization of Shh signaling proteins

Christine E. Larkins[a,b], Gladys D. Gonzalez Aviles[a], Michael P. East[b,c], Richard A. Kahn[c], and Tamara Caspary[a]

[a]Department of Human Genetics, School of Medicine, [b]Graduate Program in Biochemistry, Cell and Developmental Biology, and [c]Department of Biochemistry, School of Medicine, Emory University, Atlanta, GA 30322

ABSTRACT **Arl13b, a ciliary protein within the ADP-ribosylation factor family and Ras superfamily of GTPases, is required for ciliary structure but has poorly defined ciliary functions. In this paper, we further characterize the role of Arl13b in cilia by examining mutant cilia in vitro and determining the localization and dynamics of Arl13b within the cilium. Previously, we showed that mice lacking Arl13b have abnormal Sonic hedgehog (Shh) signaling; in this study, we show the dynamics of Shh signaling component localization to the cilium are disrupted in the absence of Arl13b. Significantly, we found Smoothened (Smo) is enriched in Arl13b-null cilia regardless of Shh pathway stimulation, indicating Arl13b regulates the ciliary entry of Smo. Furthermore, our analysis defines a role for Arl13b in regulating the distribution of Smo within the cilium. These results suggest that abnormal Shh signaling in *Arl13b* mutant embryos may result from defects in protein localization and distribution within the cilium.**

Monitoring Editor
Patrick Brennwald
University of North Carolina

Received: Dec 21, 2010
Revised: Aug 31, 2011
Accepted: Sep 26, 2011

INTRODUCTION

The regulation of protein delivery and movement within primary cilia is key to our understanding of how cilia are built and how their length is controlled, as well as how cell signaling pathways are regulated (Veland *et al.*, 2009). Ciliary length and cell signaling are both disrupted in the absence of Arl13b, a small GTPase that localizes to cilia. *Arl13b*$^{hennin\ (hnn)}$ mutant mouse embryos have cilia that are one-half the length of wild-type and a specific defect in the axoneme, where the B-tubule of the outer doublet microtubules is not connected to the A-tubule (Caspary *et al.*, 2007). In addition, these mutant embryos show a low level of expanded Shh activation in the neural tube (Caspary *et al.*, 2007). In mammals, Arl13b is one of ~30 ADP-ribosylation factor (Arf) family proteins, best known for regulatory roles in membrane trafficking and cytoskeletal dynamics (D'Souza-Schorey and Chavrier, 2006; Zhou *et al.*, 2006). Therefore defining the molecular actions of Arl13b in cilia and ciliogenesis is expected to shed light on the links between ciliary formation and signaling, with possible links to membrane traffic and/or cytoskeletal regulation.

Almost all components of the Sonic hedgehog (Shh) signaling pathway are localized to the cilium, and their localization shifts in response to the Shh ligand (Corbit *et al.*, 2005; Haycraft *et al.*, 2005; Rohatgi *et al.*, 2007; Chen *et al.*, 2009; Wen *et al.*, 2010). In the absence of ligand, the Gli transcription factors Gli2 and Gli3 are localized to the tips of cilia and are processed to form transcriptional repressors (GliRs; Haycraft *et al.*, 2005; Huangfu and Anderson, 2005; Liu *et al.*, 2005). This processing involves the phosphorylation and cleavage of the full-length Glis, with the N-terminal domain acting as the repressor and the C-terminal domain being degraded (Wang *et al.*, 2000). The receptor for the Shh ligand, Patched (Ptch1), is also found in the ciliary membrane, and represses pathway activation in the absence of ligand by inhibiting the downstream activator, Smoothened (Smo; Rohatgi *et al.*, 2007). When Shh ligand is present, Shh binds Ptch1, causing it to move out of the cilium, and this allows Smo to enter (Corbit *et al.*, 2005; Rohatgi *et al.*, 2007). Smo localization to the cilium inhibits GliR formation and, via an unknown mechanism, the full-length Glis become Gli activators (GliAs; McMahon *et al.*, 2003). Suppressor of Fused (Sufu), an inhibitor of Gli activity, is also localized to the tips of cilia, although Sufu was found to inhibit Shh signaling independently of the cilium

This article was published online ahead of print in MBoC in Press (http://www.molbiolcell.org/cgi/doi/10.1091/mbc.E10-12-0994) on October 5, 2011.

Address correspondence to: Tamara Caspary (tcaspar@emory.edu).

Abbreviations used: Arf, ADP-ribosylation factor; EYFP, enhanced yellow fluorescent protein; FBS, fetal bovine serum; FRAP, fluorescence recovery after photobleaching; GFP, green fluorescent protein; GliA, Gli activators; GliR, Gli transcriptional repressor; IFT, intraflagellar transport; MEFs, mouse embryonic fibroblasts; PBS, phosphate-buffered saline; PFA, paraformaldehyde; Ptch1, Patched; RFP, red fluorescent protein; Shh, Sonic hedgehog; shRNA, short hairpin RNA; Smo, Smoothened; Sufu, Suppressor of Fused.

© 2011 Larkins *et al.* This article is distributed by The American Society for Cell Biology under license from the author(s). Two months after publication it is available to the public under an Attribution–Noncommercial–Share Alike 3.0 Unported Creative Commons License (http://creativecommons.org/licenses/by-nc-sa/3.0).

"ASCB®," "The American Society for Cell Biology®," and "Molecular Biology of the Cell®" are registered trademarks of The American Society of Cell Biology.

by binding and sequestering the Glis in the cytoplasm (Chen *et al.*, 2009; Jia *et al.*, 2009; Humke *et al.*, 2010; Tukachinsky *et al.*, 2010).

Precisely how Shh signaling proteins are targeted and moved in and out of the cilium is not clear, but intraflagellar transport (IFT) is required (Huangfu *et al.*, 2003; Haycraft *et al.*, 2005; Liu *et al.*, 2005). IFT is the bidirectional movement of ciliary protein complexes and is required to build and maintain the cilium (Kozminski *et al.*, 1993; Rosenbaum and Witman, 2002; Pedersen *et al.*, 2008). Anterograde IFT carries cargo toward the tip of the cilium, while retrograde transport carries turnover products out of the cilium; deletion of anterograde or retrograde IFT proteins results in distinct ciliary phenotypes, but in either case, both GliA and GliR are affected, resulting in disrupted Shh activity (Huangfu *et al.*, 2003; Huangfu and Anderson, 2005; Liu *et al.*, 2005; May *et al.*, 2005; Houde *et al.*, 2006; Ocbina and Anderson, 2008; Tran *et al.*, 2008; Cortellino *et al.*, 2009).

Surprisingly, disruption of ciliary structure does not always affect Shh signaling, as shown by *Rfx3* mouse mutants, which have short cilia and normal Shh activity (Bonnafe *et al.*, 2004). This underscores the ill-defined nature of the mechanisms by which a growing list of ciliary/basal body protein mutants affect Shh signaling (Ferrante *et al.*, 2006; Vierkotten *et al.*, 2007; Norman *et al.*, 2009; Patterson *et al.*, 2009; Boehlke *et al.*, 2010). *Arl13b*^{hnn} mutants are unusual, because the production and/or function of only GliA, and not GliR, is affected in these mutants (Caspary *et al.*, 2007). In this study, we examine what could link all these threads: a small regulatory GTPase, a specific anomaly in the ciliary ultrastructure, and the unique defect in Shh signaling. We investigate the ciliary function of Arl13b by examining its localization, dynamics, and regulation of ciliary structure. Further, we show that many Shh signaling pathway components are mislocalized in the absence of Arl13b, suggesting a general role for Arl13b in protein trafficking to the cilium.

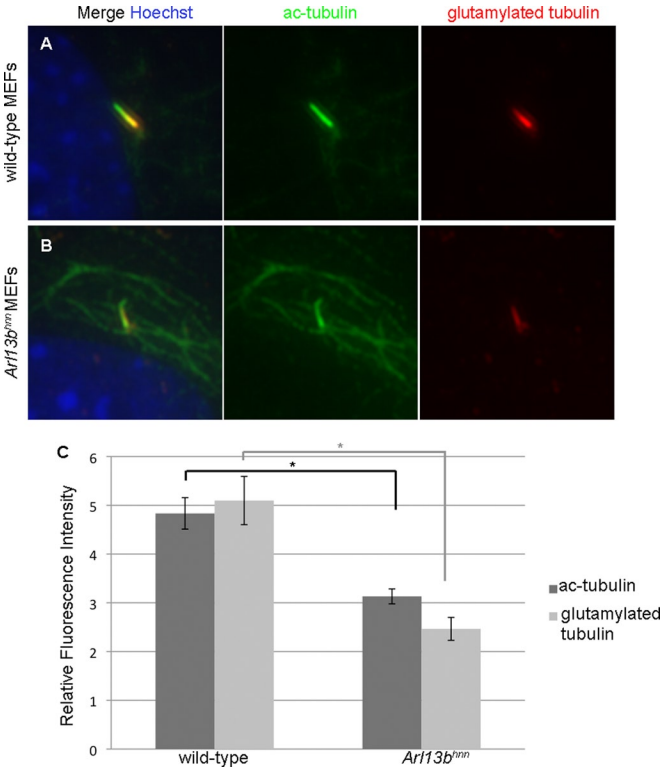

FIGURE 1: Tubulin modification defects in *Arl13b*^{hnn} mutant MEFs. (A and B) Immunofluorescence for acetylated α-tubulin (ac-tubulin; green) and glutamylated tubulin (red) in wild-type (A) and *Arl13b*^{hnn} (B) MEFs shows reduced staining for both antibodies in *Arl13b*^{hnn} MEFs. (C) Quantification of the average fluorescence intensity of acetylated α-tubulin and glutamylated tubulin fluorescence relative to background staining. Error bars are ± SEM. *p < 0.0001 using Student's *t* test.

RESULTS

Defects in posttranslational modifications of ciliary tubulin are consistent with defects in the architecture of *Arl13b*^{hnn} cilia

Arl13b^{hnn} mutant mouse embryos display shortened cilia and an ultrastructural defect, whereby the B-tubule of the microtubule-based outer doublets does not connect to the A-tubule (Caspary *et al.*, 2007). Zebrafish and *Tetrahymena* mutants with defects in tubulin glutamylation display a similar phenotype in the outer doublets (Redeker *et al.*, 2005; Pathak *et al.*, 2007; Dave *et al.*, 2009). To examine such posttranslational modifications in the axoneme of *Arl13b*^{hnn} cilia, we derived primary mouse embryonic fibroblasts (MEFs) from e12.5 *Arl13b*^{hnn} and wild-type embryos. Using immunofluorescence, we examined tubulin glutamylation by measuring the average fluorescence intensity along the entire cilium relative to background staining. We saw a significant reduction in staining of the *Arl13b*^{hnn} axoneme compared with wild-type (Figure 1, A–C).

We then extended these analyses to another tubulin posttranslational modification, acetylation. Although the functional significance of tubulin acetylation is less clear, the ciliary axoneme is highly acetylated and is predicted to be a mark of stable microtubules (Perdiz *et al.*, 2010). We found tubulin acetylation is reduced to similar levels as glutamylation in *Arl13b*^{hnn} MEFs (Figure 1, A–C), indicating a more general defect in tubulin posttranslational modifications in our mutants.

Arl13b regulates ciliary length

To further investigate the role of Arl13b in ciliogenesis, we examined cilia in cultured wild-type and *Arl13b*^{hnn} MEFs. Of wild-type MEFs, 71.7% were ciliated, whereas 19.0% of *Arl13b*^{hnn} MEFs had cilia (Figure 2A). In contrast, all cells of the *Arl13b*^{hnn} embryonic node are ciliated (Caspary *et al.*, 2007). However, reminiscent of what we found in vivo, the *Arl13b*^{hnn} MEF cilia were shorter than wild-type cilia, suggesting Arl13b controls ciliary length both in the embryo and in culture (Figure 2, C, D, and M).

To unravel how Arl13b might regulate ciliary length, we examined cilia in MEFs overexpressing untagged Arl13b or Arl13b-green fluorescent protein (GFP). We found wild-type MEFs overexpressing untagged Arl13b or Arl13b-GFP had much longer cilia than untransfected cells, and both constructs rescued the ciliary length defect in *Arl13b*^{hnn} MEFs (Figure 2, B, E–H, and M). The rescued cilia were longer than wild-type, consistent with Arl13b protein levels being important. The cilia in wild-type or *Arl13b*^{hnn} MEFs overexpressing Arl13b-GFP were shorter than those expressing untagged Arl13b, indicating the C-terminal GFP tag impaired Arl13b's function, consistent with previous observations with tagged versions of Arf GTPases (Jian *et al.*, 2010). In the few cases where Arl13b-GFP was restricted from the cilium and instead was evident throughout the cell body and nucleus, there was no change in ciliary length, suggesting Arl13b needs to be in the cilium to regulate ciliary length (Figure 2M).

Of the 30 mammalian Arf family proteins, most are ~20-kDa proteins consisting of the Arf domain only (D'Souza-Schorey and Chavrier, 2006; Kahn *et al.*, 2006). Arl13b is unusual in that it has an additional 24-kDa novel C-terminus, much of which its nonvertebrate orthologues lack. We examined the localization

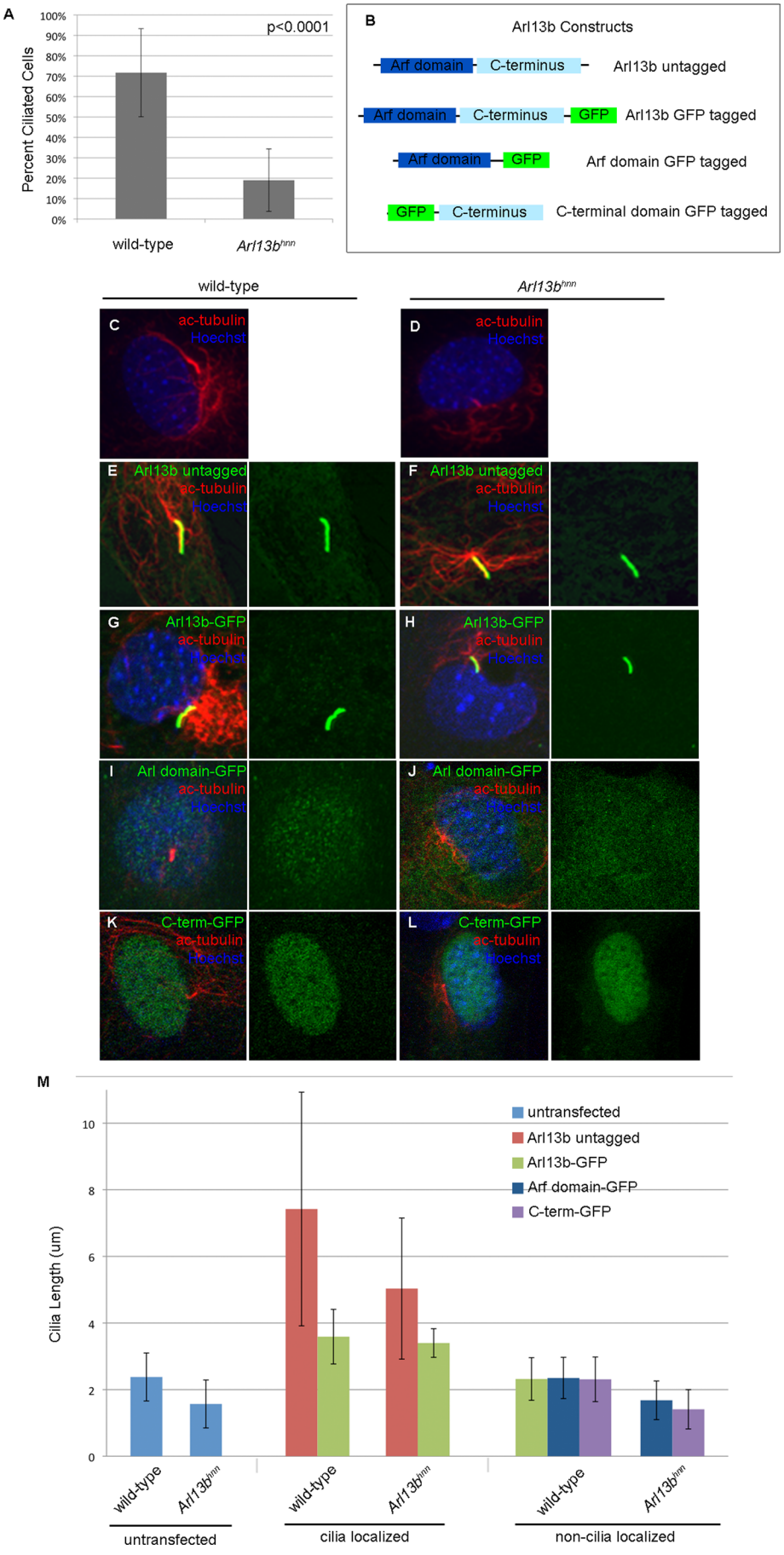

and function of the Arf domain and the novel C-terminal domain by tagging each with GFP and expressing each in wild-type and *Arl13b*^{hnn} MEFs. Neither half of Arl13b could localize to cilia as the full-length version did; we found the tagged Arf domain in diffuse puncta within the cell body and the tagged C-terminal domain in the nucleus (Figure 2, I–L). Furthermore, neither half of Arl13b had any effect on ciliary length in wild-type or *Arl13b*^{hnn} MEFs, consistent with our finding that full-length Arl13b-GFP regulated ciliary length only when it was in cilia (Figure 2M). Thus, only full-length Arl13b localizes to cilia to regulate ciliary length.

Arl13b localizes to the ciliary membrane

We previously demonstrated that Arl13b is expressed in cilia and does not overlap with the basal body in fibroblasts (Caspary *et al.*, 2007). To define where in the cilium Arl13b localizes, we took advantage of the long cilia in the mouse kidney cell line IMCD3 and used immunofluorescence. As in the fibroblasts, Arl13b was visible along the entire length of the cilium, but did not colocalize with the basal body marker γ-tubulin (Figure 3, A and C). To determine whether Arl13b within the cilium associates with the membrane or the axoneme, we treated cells with the detergent TritonX-100 prior to fixation. We saw a loss of Arl13b staining in TritonX-100-treated cells, but acetylated α-tubulin staining remained intact, suggesting the majority of Arl13b is not associated with the axoneme (Figure 3, A–D). We also saw that the known ciliary membrane protein SSTR3 fused with GFP

FIGURE 2: Arl13b regulates ciliary length. (A) Quantification of the percent of ciliated cells in wild-type and *Arl13b*^{hnn} MEFs. (B) Schematic of the Arl13b constructs that were transfected into MEFs. (C and D) Immunofluorescence for acetylated α-tubulin (ac-tubulin) in wild-type and *Arl13b*^{hnn} MEFs shows shortened cilia in *Arl13b*^{hnn} MEFs. (E–L) Immunofluorescence for GFP and acetylated α-tubulin in wild-type and *Arl13b*^{hnn} MEFs expressing GFP-tagged Arl13b constructs. (M) Quantification of ciliary length in MEFs with and without transfection. The constructs are separated by those that localize to cilia and those that do not. Error bars are ± SD. For untransfected wild-type vs. *Arl13b*^{hnn} MEFs, $p < 0.0001$. For wild-type vs. wild-type–overexpressing Arl13b-GFP and untagged Arl13b in the cilium, $p < 0.0001$; for *Arl13b*^{hnn} vs. *Arl13b*^{hnn} overexpressing Arl13b-GFP and untagged Arl13b, $p < 0.0001$.

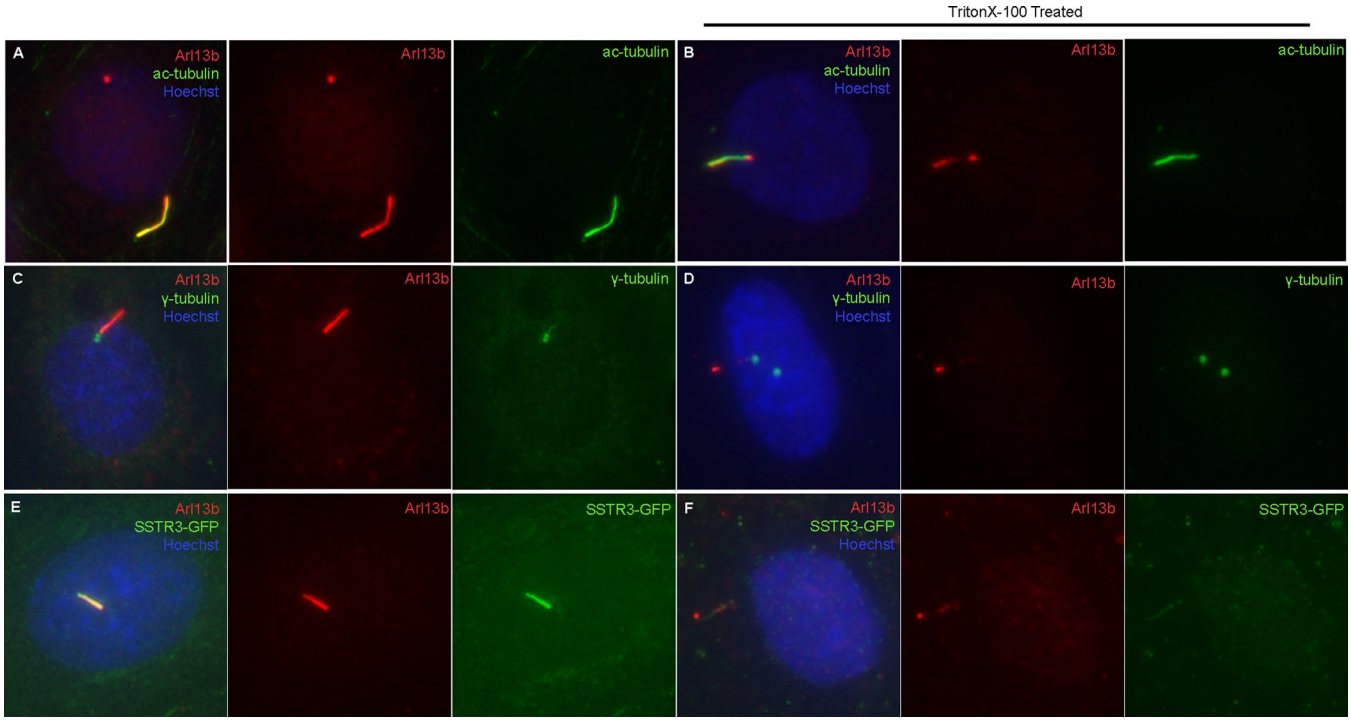

FIGURE 3: Ciliary Arl13b is TritonX-100 soluble. (A and C) Immunofluorescence in IMCD3 cells shows that Arl13b colocalizes with the ciliary marker acetylated α-tubulin (A) and does not colocalize with the basal body marker γ-tubulin (C). (B and D) Triton X-100 treatment results in the loss of a majority of Arl13b staining in the cilium, although axoneme staining with acetylated α-tubulin remains (B). (E and F) The known ciliary membrane protein SSTR3-GFP shows a similar loss of ciliary staining with TritonX-100 treatment (F).

(SSTR3-GFP) was lost upon pretreatment with detergent, consistent with Arl13b being membrane associated (Figure 3, E and F). Curiously, we saw that Arl13b staining remained at the base and tip of the cilium after detergent treatment prior to fixation, which we did not observe with SSTR3-GFP. This suggests that some Arl13b is anchored to the axoneme ends or other machinery found at the base and tip of the cilium. It could also be an indication that the membrane of the base and tip of the cilium is less detergent soluble, as is the case for lipid raft domains.

We next used fluorescence recovery after photobleaching (FRAP) to determine the dynamics of Arl13b movement within the cilium of IMCD3 cells. To do this, we generated a lentivirus capable of driving expression of Arl13b-GFP and infected IMCD3 cells. When we photobleached the central region of the cilium, we saw rapid recovery of Arl13b-GFP fluorescence in the bleached region (Figure 4, A and C). We performed the parallel analysis with SSTR3-GFP (Figure 4, B and C) and found the same rates of recovery for Arl13b-GFP and SSTR3-GFP (Figure 4C). To determine Arl13b turnover within the cilium, we photobleached Arl13b-GFP as well as SSTR3-GFP in the entire cilium and saw very little recovery of either protein over the course of the experiment, which we followed for 2 min 23 s (Figure 4, D, E, and G). In contrast, in a parallel analysis performed by photobleaching IFT88-EYFP–expressing cells, we saw a faster rate of recovery (Figure 4, F and G), consistent with previous data showing that IFT recovery in the cilium is faster than the recovery of ciliary membrane proteins (Hu *et al.*, 2010). Taken together, these data are consistent with Arl13b associating with the membrane of the cilium.

IFT appears normal in the absence of Arl13b

As IFT is the major transport machinery that builds cilia, we wanted to further investigate the relationship between Arl13b and IFT and test whether Arl13b regulates IFT in mammalian cells. We took advantage of an IMCD3 cell line that stably expressed IFT88-EYFP, which enabled us to perform FRAP and measure the rate of IFT88-EYFP recovery. To deplete the cells of Arl13b, we used a lentivirus coexpressing Arl13b short hairpin RNA (shRNA) and red fluorescent protein (RFP), enabling us to specifically identify knockdown cells. We proved the knockdown was efficient by Western blotting, as we detected only 30% of the wild-type Arl13b levels in cells treated with the knockdown virus (Figure 5A). Arl13b was not detected by immunofluorescence in 50% of RFP-positive cells, and the phenotype was similar to what we found in the Arl13b-null MEFs: 50% fewer cilia, and those that were present were shortened (Figure 5, B, C, and E). When we measured the rate of recovery of IFT88-enhanced yellow fluorescent protein (EYFP) at the ciliary tip, we saw no significant change between IMCD3 wild-type and Arl13b knockdown cells (Figure 5H). Because the knockdown is sufficient to reflect the established Arl13b ciliary phenotype, the simplest interpretation is that Arl13b is not required for nor does it provide essential regulation of the rate of IFT. Nevertheless, we cannot rule out such a function, as some Arl13b remains after knockdown.

Dynamic localization of Shh signaling proteins is disrupted in *Arl13b*^{hnn} MEFs

Arl13b functions in the cilium to regulate Shh signaling, because Arl13b mutants that lack cilia (*Arl13b*^{hnn} *IFT172*^{wim} double mutant embryos), like *IFT172*^{wim} mutant embryos that lack cilia completely, display no Shh response (Caspary *et al.*, 2007). However, in contrast to most ciliary mutants in mouse, *Arl13b*^{hnn} single mutant embryos have a low level of ligand-independent Shh pathway activation in the neural tube, due to a specific disruption in GliA activity (Caspary *et al.*, 2007). Since the goal of Shh signaling is to control the balance

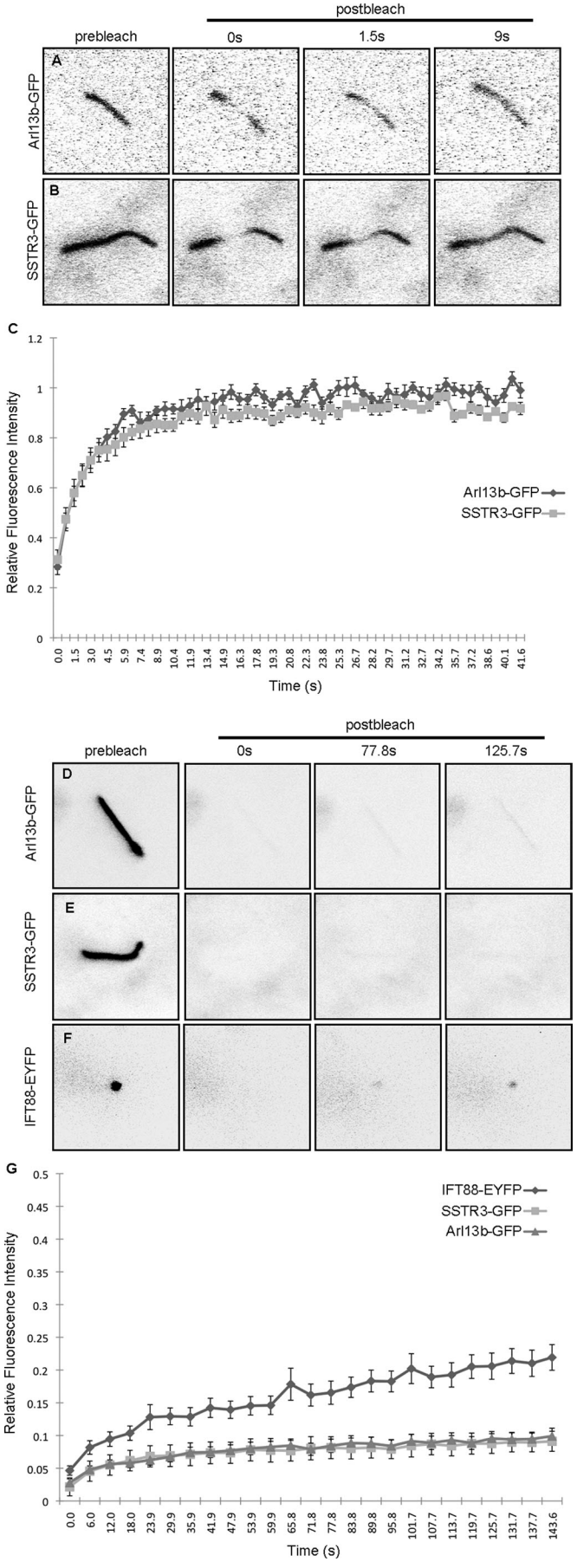

of GliA and GliR, and this balance requires cilia, we investigated Shh signaling and the localization of Shh components to the cilia of *Arl13b*^{hnn} mutant MEFs with and without Shh stimulation.

First, we sought to monitor Shh activity in wild-type and *Arl13b*^{hnn} MEFs. We therefore cotransfected a firefly luciferase reporter construct with eight Gli-binding sites in its promoter (8×Gli luciferase) with a *Renilla* luciferase expression construct to control for transfection efficiency in wild-type and *Arl13b*^{hnn} MEFs (Sasaki *et al.*, 1997). The levels of normalized luciferase activity in untreated wild-type and *Arl13b*^{hnn} MEFs were similar (Figure 6A). When treated with Shh-conditioned media, wild-type MEFs showed almost a sevenfold increase in normalized luciferase activity, whereas *Arl13b*^{hnn} MEFs displayed only a twofold increase, indicating *Arl13b*^{hnn} cells have a lowered response to the Shh ligand (Figure 6A). Because there is also a reduction of ciliated cells in *Arl13b*^{hnn} mutant cilia, it is difficult to determine whether the reduced Shh response is caused by a reduction in cilia or by defective Shh signaling in the ciliated *Arl13b*^{hnn} cells or by both.

To better determine the Shh response within only the ciliated *Arl13b*^{hnn} mutant cells, we examined the dynamics of Shh components using antibodies against the endogenous proteins. Normally, Gli2 and Gli3 localize to the ciliary tip and are further enriched there after Shh stimulation (Chen *et al.*, 2009; Wen *et al.*, 2010). Indeed, when we measured the fluorescence intensity in the tips of cilia relative to background staining using antibodies that recognize full-length Gli2, the N-terminal domain of Gli3 (Gli3N) or the C-terminal domain of Gli3 (Gli3C), we found Gli2 and Gli3 were enriched in wild-type MEFs after treatment with Shh-conditioned media (Figure 6, B, D, F, and N; Wen *et al.*, 2010). Interestingly, there was no significant change in Gli2 and Gli3 enrichment in *Arl13b*^{hnn} MEFs after Shh treatment (Figure 6, C, E, G, and N). Similarly, we confirmed that Sufu, a mediator of Gli function, shows enrichment in the tips of cilia after Shh treatment in wild-type, but not *Arl13b*^{hnn}, MEFs (Figure 6, H, I, and N).

Smo and Ptch1 localize along the length of the cilium in a complementary manner: Ptch1 in the absence of ligand and Smo upon pathway stimulation (Corbit *et al.*, 2005; Rohatgi *et al.*, 2007). As expected, we saw Ptch1 ciliary levels decrease and Smo ciliary levels increase after Shh stimulation in wild-type MEFs (Figure 6, J, L, and N). We investigated how these dynamics changed in the absence of Arl13b and found Ptch1 staining did not significantly change in response to Shh stimulation in *Arl13b*^{hnn} MEFs (Figure 6, L–N). Interestingly, we found Smo localized to the cilium in *Arl13b*^{hnn} MEFS without Shh stimulation (Figure 6, J, K, and N), indicating Arl13b

FIGURE 4: Arl13b-GFP dynamics reflect those of a ciliary membrane protein. The figure shows overexposed images for viewing purposes, but all intensities were measured without overexposure of pixels. (A and B) Photobleaching of a region of Arl13b-GFP (A) in the center of the cilium shows recovery dynamics similar to SSTR3-GFP (B). (C) Quantification of the recovery dynamics for SSTR3-GFP and Arl13b-GFP shows no significant difference in the recovery curve (prior to 5.9 s, $p > 0.3$ using Student's *t* test). The relative fluorescence intensity was quantified as the intensity in the bleached region relative to the whole cilium. (D to G) Photobleaching Arl13b-GFP (D) and SSTR3-GFP (E) in the whole cilium results in little fluorescence recovery (G). IFT88-YFP has a faster recovery rate in the cilium (F and G); $p < 0.02$ for both Arl13b-GFP and SSTR3-GFP, compared with IFT88-YFP at 29.9 s. (G) Quantification of fluorescence intensity is determined as the intensity of the bleached region (cilium) relative to an unbleached region in the field. All experiments were corrected for background. Error bars are ± SEM (C and G).

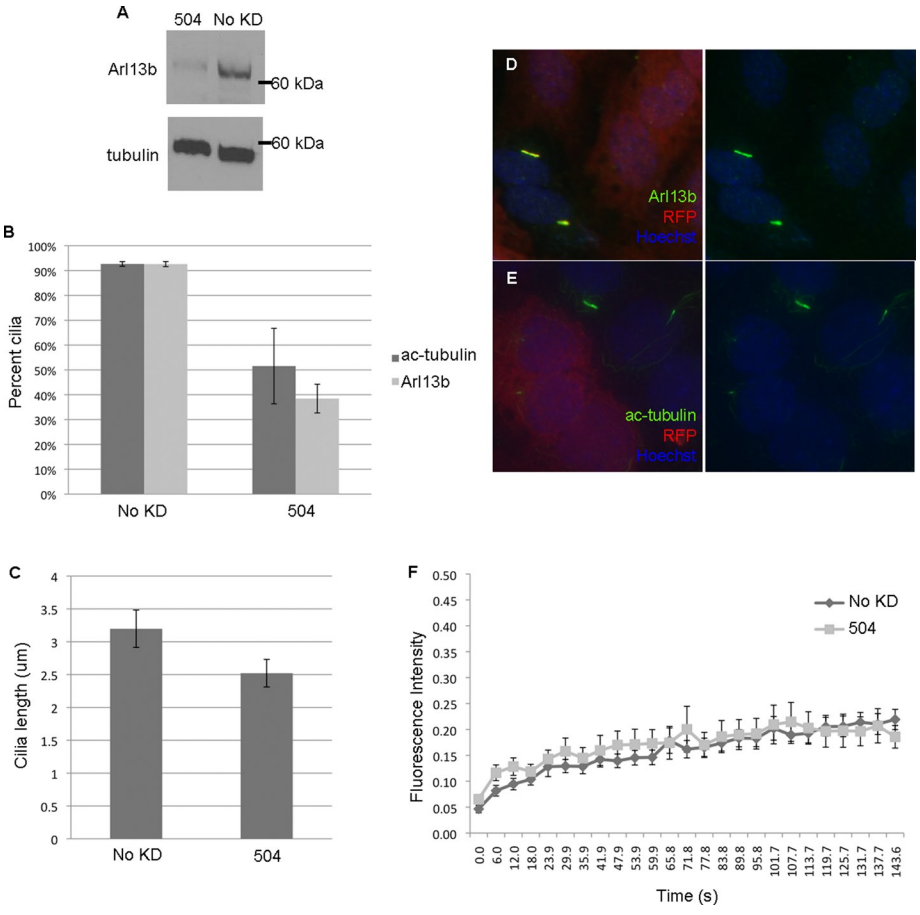

FIGURE 5: IFT88 recovery is intact in *Arl13b* mutant cells. (A) Western blot showing knockdown of Arl13b in IMCD3 cells. (B) Quantification of the percentage of cells showing cilia stained with acetylated α-tubulin and Arl13b. (C) Quantification of ciliary length in knockdown cells compared with no knockdown. (D and E) Immunofluorescence for (D) Arl13b and (E) acetylated α-tubulin (ac-tubulin) costained with RFP in cells expressing the 504 knockdown construct. (F) Recovery of IFT88-EYFP in IMCD3 cells with and without knockdown of Arl13b. Error bars are ± SEM (C and F) and ± SD (B).

these results indicate an important role for Arl13b in length control. Additionally, we found abnormal tubulin modifications in mutant cilia, consistent with the structural defect in the axoneme that may contribute to ciliary shortening, which supports a role for Arl13b in regulating tubulin modifications within the cilium. Furthermore, we found the dynamics of many Shh signaling components were disrupted, with defective Smo localization within the cilium, showing the importance of Arl13b in Shh signaling protein localization. Although these results may imply that Arl13b has multiple independent functions in ciliary biology, they could also indicate a singular function of Arl13b that affects these various aspects of ciliary biology, such as a role in protein trafficking to and within the cilium that, when disrupted, results in defects in ciliary length, tubulin modifications, and protein localization to the cilium.

The role of Arl13b in ciliogenesis

We showed that loss of Arl13b led to shortened cilia and reduced numbers of cilia in vitro, while overexpression of Arl13b caused increased ciliary length. Many different ciliary proteins have been associated with ciliary length regulation, and most of these proteins point to steady-state protein trafficking to and from cilia as being the ultimate regulator of ciliary length (Ishikawa and Marshall, 2011). Interestingly, the closely related GTPase Arl6 recruits trafficking proteins of the Bardet-Biedl syndrome complex to the cilium and regulates ciliary length (Jin *et al.*, 2010; Wiens *et al.*, 2010). We therefore think it is likely that Arl13b also plays a similar role in controlling protein trafficking to or from the cilium, or both.

Our findings that Arl13b is solubilized from cilia with detergent and moves within the cilium with dynamics almost identical to the ciliary intrinsic membrane protein SSTR3 are consistent with Arl13b forming a quite stable association with cell membranes through N-terminal palmitoylation, as demonstrated in 293T cells (Cevik *et al.*, 2010). Furthermore, these dynamics fit with evidence that ciliary membrane proteins have very long half-lives within the cilium (Hu *et al.*, 2010). It is interesting that IFT proteins are tightly associated with the ciliary membrane while being transported along the axoneme and that the Arl13b *Caenorhabditis elegans* orthologue ARL13 stabilizes IFT (Pigino *et al.*, 2009; Cevik *et al.*, 2010). However, we did not see a defect in IFT recovery using our FRAP method to examine IFT dynamics in *Arl13b* knockdown cells, which could be reflective of our method or could indicate that the vertebrate orthologue of Arl13b does not regulate IFT. Other methods to examine IFT and to determine protein interactors will be crucial for establishing whether Arl13b plays a role in regulating IFT.

The ~24-kDa C-terminal domain of Arl13b is critical to its function. The domain is vertebrate-specific and required for Arl13b localization to cilia, and we found that tagging it with GFP reduces the ability of Arl13b to regulate ciliary length. The fact that the C-terminal domain of Arl13b localizes to the nucleus when GFP-tagged is

plays a critical role in regulating the entry of Smo into cilia. We found Smo was further enriched on Shh stimulation in *Arl13b*^{hnn} MEFS (Figure 6, K and N). However, regardless of whether or not the cells were stimulated, Smo was found enriched in large puncta in the cilia lacking Arl13b, in contrast to the more evenly distributed Smo staining in wild-type MEF cilia (Figure 6, J and K), arguing that Arl13b also regulates the proper localization or targeting of Smo within the cilium. In *Arl13b*^{hnn} MEFs without Shh stimulation, Smo staining was most often concentrated in a single puncta at either the ciliary tip (31.8% of cells), in the proximal cilium (11.4%), in the center of the cilium (13.6%), or in two or three puncta in multiple regions of the cilium (22.7%). After treatment of the cells with Shh-conditioned medium, *Arl13b*^{hnn} MEFs showed a shift in the localization of ciliary Smo such that more cells had multiple sites of concentrated Smo (37.8%). In sum, these results demonstrate a fundamental defect in the trafficking of Shh signaling proteins in *Arl13b*^{hnn} MEFs.

DISCUSSION

Our data here point to an essential role for Arl13b in multiple aspects of ciliogenesis and ciliary protein localization. We saw that cell lines with disrupted Arl13b expression have reduced numbers of cilia, and those cilia that are present are shorter, whereas cells overexpressing Arl13b show increased ciliary length. Taken together,

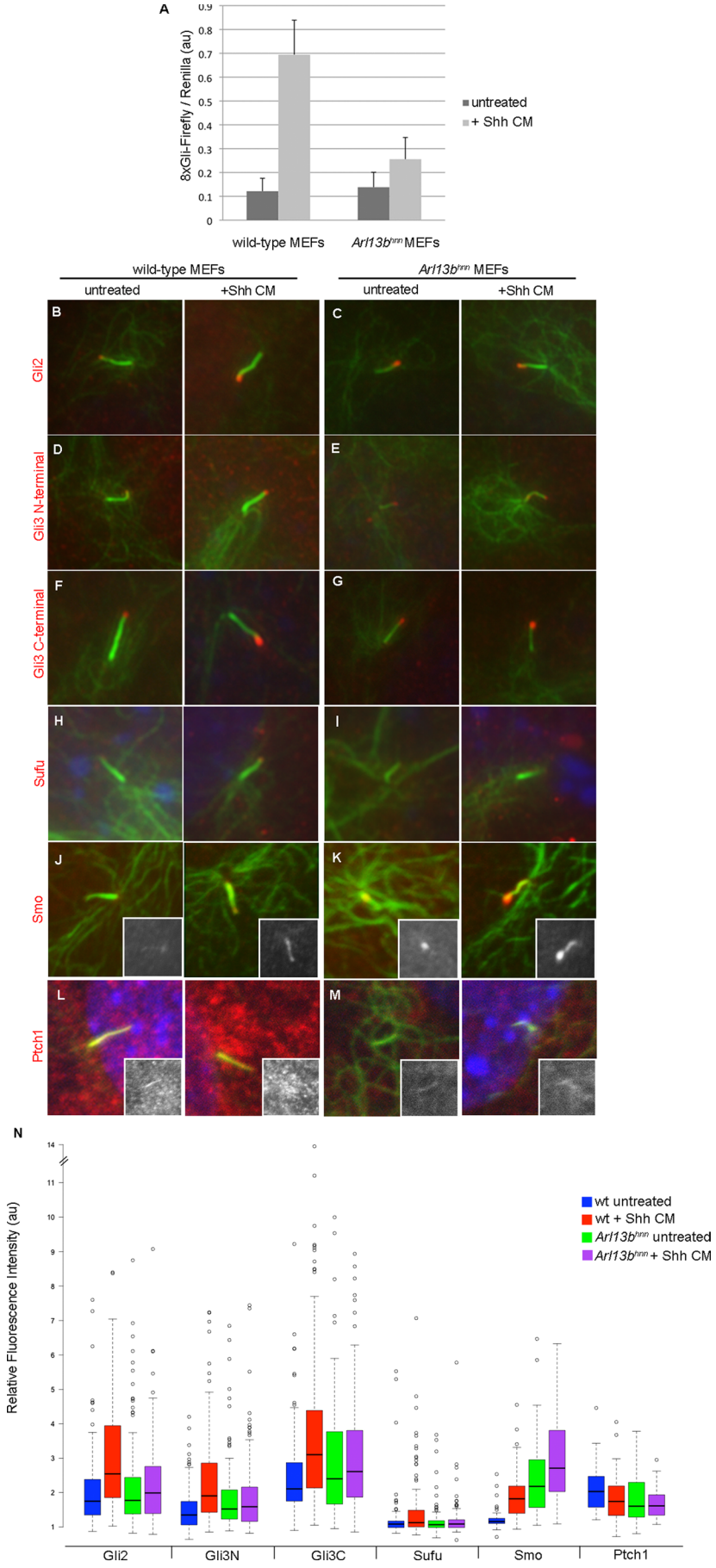

interesting, since it contains a basic sequence that may act as a nuclear localization signal. Recent data demonstrated that a similar sequence in the C-terminus of Kif17 mediates ciliary localization and that a truncated Kif17 lacking its N-terminus also localizes to the nucleus (Dishinger *et al.*, 2010). In addition, importin-β has been localized to cilia and is required for ciliary entry of some proteins (Fan *et al.*, 2007; Dishinger *et al.*, 2010), raising the possibility that Arl13b localizes to cilia through an importin-β interaction domain in its C-terminus. As the N-terminus of Arl13b contains palmitoylation sites (Cevik *et al.*, 2010), interactions with vesicles or periciliary membrane may be required for ciliary versus nuclear localization.

While the reduction of both acetylation and glutamylation in *Arl13b*^{hnn} cilia is consistent with the architectural defect of the axoneme (Pathak *et al.*, 2007; Pugacheva *et al.*, 2007), we cannot say whether the modification defects we see are the result or the cause of a potential defect in protein trafficking to cilia. Interestingly, in *C. elegans*, the Arl13 mutant phenotype is rescued by loss of Arl3 function, and loss of Arl3 increases tubulin acetylation in HeLa cells (Zhou *et al.*, 2006; Li *et al.*, 2010), indicating these two proteins may have inverse functions in regulating tubulin modifications. Examining a potential Arl3 and Arl13b interaction in mammalian cells will be important for teasing apart these possibilities.

The role of Arl13b in Shh signaling

Arl13b^{hnn} mutant embryos display defects in Shh signaling in the neural tube, such that there is a ligand-independent expansion of Shh signaling activity, while the highest levels of activity are not reached in the ventral neural tube (Caspary *et al.*, 2007). To begin to investigate this signaling defect, we examined Shh signaling in *Arl13b*^{hnn} MEFs. For our initial investigation, we determined the Shh signaling response in

FIGURE 6: Shh signaling component localization is disrupted in *Arl13b*^{hnn} MEFs. (A) Quantification of Gli-luciferase activity relative to *Renilla* luciferase. (B–M) Immunofluorescence for acetylated α-tubulin (green) and Gli2, Gli3, Sufu, Smo, and Ptch1 (red). In wild-type MEFs (B, D, F, H, J, and L) Gli2, Gli3, and Sufu are enriched after Shh-conditioned media treatment, while Ptch1 levels are reduced. *Arl13b*^{hnn} MEFs (C, E, G, I, K, and M) do not show significant enrichment of Gli2, Gli3, Sufu, or Smo, and Ptch1 staining is not significantly reduced after Shh-conditioned media treatment. Insets in (J–M) are showing Ptch1 and Smo staining alone in grayscale. (N) Quantification of average fluorescence intensity in the tip of the cilium (Gli2, Gli3, and Sufu) or the entire cilium (Ptch1 and Smo) relative to cell body staining. Data from all experiments are shown. $p < 10^{-7}$ for wild-type MEFs with conditioned media vs. untreated wild-type MEFs using the Gli and Smo antibodies; $p < 0.05$ using the Ptch1 and Sufu antibodies; $p < 0.04$ for Smo staining in *Arl13b*^{hnn} MEFS with conditioned media vs. untreated *Arl13b*^{hnn} MEFS; $p < 0.04$ for Ptch1 intensities in untreated wild-type MEFs vs. untreated *Arl13b*^{hnn} MEFs.

Arl13b^{hnn} MEFs using an 8×Gli luciferase assay and saw that, without Shh treatment, mutant MEFs had levels of Shh response similar to wild-type MEFS; however, there was a defect in mutant cells responding to the Shh ligand. This result differs from what we found in *Arl13b*^{hnn} mutant embryos, in that there is a ligand-independent activation of Shh signaling in the neural tube, although the highest levels of Shh signaling cannot be reached (Caspary *et al.*, 2007). We predict that this discrepancy may be due to the number of ciliated cells found in vivo versus in vitro, as all cells appear to be ciliated in *Arl13b*^{hnn} embryos, whereas less than one-half of the cells are ciliated in *Arl13b*^{hnn} MEFs (Caspary *et al.*, 2007). Given that loss of cilia in *Arl13b*^{hnn} mutants causes loss of Shh signaling (Caspary *et al.*, 2007), this could explain the lowered response to Shh in the population of *Arl13b*^{hnn} MEFs.

We next examined the localization of Shh signaling components in the cilia of *Arl13b*^{hnn} MEFs using antibodies to endogenous proteins. The defects in Shh component localization we found were more consistent with the phenotype in the *Arl13b*^{hnn} mutant neural tube, perhaps because we were able to focus on only the ciliated cells in the population. First, we showed that Gli2 and Gli3 were not properly enriched at the ciliary tip when *Arl13b*^{hnn} MEFs were stimulated with Shh-conditioned media. Similarly, there was a defect in shifting Sufu localization in *Arl13b*^{hnn} MEFs in response to Shh-conditioned media. These results are reminiscent of the inability to reach the highest levels of Shh signaling activity in the *Arl13b*^{hnn} mutant neural tube, as it was shown previously that Gli localization to cilia is required for pathway activation (Tukachinsky, 2010). Next we found Smo was enriched in cilia in the absence of Shh stimulation and, consistent with this enrichment, we saw reduced Ptch1 staining in the cilium. The enriched ciliary Smo was unlikely to be fully active, because the Gli proteins were not properly enriched. As there is ligand-independent activation of Shh signaling in the neural tube, we would expect the enriched Smo in *Arl13b*^{hnn} cilia to show a low level of activity that allows for ligand-independent activation of the pathway.

The results presented here suggest that the relative levels of Shh signaling proteins in cilia, as well their trafficking into and out of the cilium, are important for activation and repression of the pathway, and studies of other ciliary mutants support this model. For example, the Rab23 mutant mouse has excess activation of the Shh signaling pathway in the neural tube (Eggenschwiler *et al.*, 2001), and Rab23 mutant cells were shown to have increased trafficking of Smo into the cilium (Boehlke *et al.*, 2010). However, our analysis of Arl13b argues that Smo simply being present in cilia is not sufficient for the range of Shh response. This is supported by research examining the retrograde ciliary dynein mutant, which also has enriched Smo in cilia, but reduced levels of Shh pathway activity in the neural tube (Ocbina *et al.*, 2011). Examination of these mutants and our data suggest there is a balance between Shh signaling protein localization and trafficking of signaling proteins into and out of the cilium that is important for achieving the correct levels of Shh response. Further examination of the puncta of Smo we see in the absence of Arl13b will likely provide the fundamental explanation for the inability of *Arl13b*^{hnn} embryos to reach high levels of Shh activation by defining the role of Arl13b in Smo localization within the cilium. Future studies are left to examine the mechanism of Shh signaling component interactions in the cilium to better explain how relative levels of Shh signaling proteins in cilia regulate the pathway.

MATERIALS AND METHODS

Generation of MEFs

E12.5 mouse embryos were dissected, and the head and visceral organs were removed. The embryos were then washed in clean phosphate-buffered saline (PBS), and single embryos were each transferred to a 1-ml syringe. The embryos were passed through an 18-G needle multiple times in DMEM (high glucose, 10% fetal bovine serum [FBS], penicillin, streptomycin) and transferred to a gelatinized 10-cm tissue culture dish. After the cells reached confluency, they were split 1:5. Cells were not used after passage 4.

Immunofluorescence

Cells were grown on coverslips and fixed 10 min in 4% paraformaldehyde (PFA) in PBS, then washed in antibody wash buffer (PBS, 0.1% TritonX-100, 1% heat-inactivated goat serum) for 10 min at room temperature. Primary antibodies were incubated overnight at 4°C, and after a series of washes, they were incubated in secondary antibody for 1 h at room temperature. After a second series of washes, coverslips were mounted on slides with ProLong Gold antifade reagent (Invitrogen, Carlsbad, CA). Antibodies and dilutions were as follows: Ptch1 (1:250; Raj Rahatgi, Stanford University, Stanford, CA), Smo (1:500; Kathryn Anderson, Sloan-Kettering Institute, New York, NY), acetylated α-tubulin (1:2500; T-6793, Sigma-Aldrich, St. Louis, MO), γ-tubulin (1:1000; T-6557, Sigma), Gli2 (1:2000; Jonathan Eggenschwiler, Princeton University, Princeton, NJ), Gli3C and Gli3N (2 µg/ml; Suzie Scales, Genentech, San Francisco, CA; Wen *et al.*, 2010), polyclonal GFP (1:500, AB3080, Millipore, Billerica, MA), monoclonal GFP (1:500, MAB3580, Chemicon), Sufu (1:100, SC-10933, Santa Cruz Biotechnology, Santa Cruz, CA), glutamylated tubulin (GT335, Carsten Janke, Curie Institute, Paris), and Arl13b (1:1500).

Fluorescence intensities were measured using ImageJ software, and were normalized to cell-body staining. All cilia in a field were measured, and cilia were selected in the acetylated α-tubulin channel to prevent biased selection. For all antibodies except Gli2, Gli3 C-terminal, Gli3 N-terminal, and Sufu, the average intensity in the entire cilium was measured relative to background. For the Glis and Sufu, which only stain the tips of cilia, the fluorescence intensity in only the tip was measured relative to background. The tip of the cilium was determined by weakened acetylated α-tubulin staining, as well as orientation. Three independent experiments were performed for all antibodies, and a total of at least 125 cilia were measured for the Gli and Sufu antibodies, and at least 40 cilia were measured for all other antibodies. Significance was determined for all experiments using a one-tailed Student's *t* test. Smo and Ptch1 antibodies were imaged on a Zeiss LSM510 META (Carl Zeiss Microscopy, Thornwood, NY) confocal at 63× with optical zoom. All other antibodies were imaged on a Leica DM6000B (Leica Microsystems, Buffalo Grove, IL) upright microscope at 100× with SimplePCI software (Hamamatsu Corp., Sewickley, PA).

For removal of the ciliary membrane, cells were treated with 0.1% TritonX-100 in PBS without Ca^{2+} or Mg^{2+} for 1 min and then fixed in 4% PFA. Antibody staining was then performed as described in the preceding paragraphs.

FRAP

IMCD3 cells were transduced with a viral construct expressing Arl13b-GFP. All cells were grown to confluency. SSTR3-GFP cells were from Greg Pazour and IFT88-YFP cells were from Brad Yoder. FRAP was performed on a Zeiss LSM510 META confocal using 63× objective with optical zoom. Briefly, cilia were photobleached using the 488-nm laser with 25 iterations at 50% power. Images were scanned at 3% laser power. Fluorescence intensity measurements had background subtracted, and the bleached region was normalized to the entire cilium (for determination of movement within the

cilium) or to an unbleached region in the same field (for determination of turnover in the cilium).

Shh-conditioned media

Conditioned medium was generated as previously described (Taipale *et al.*, 2000). Briefly, 293 EcR Shh cells (ATCC; CRL-2782) were grown to confluence, and 1 μM of MurA was added to the cells in 2% serum DMEM. After 24 h, the conditioned medium was collected and the 2% serum MurA media was replaced. A collection was taken again after 24 h, and that medium was combined with the first collection.

For immunofluorescence of MEFs treated with Shh-conditioned media, cells were plated at 800,000 cells per well of a six-well plate. At confluence, cells were serum-starved in DMEM high glucose with 0% serum. After 24 h of serum-starving, conditioned medium diluted 1:4 was added to the cells. Untreated control cells were given 0.5% serum media at this point. After 24 h of treatment, the cells were harvested for immunofluorescence.

Knockdown construct

The knockdown viral construct was generated using Sigma's Mission custom viral vector synthesis. The vector, clone ID, and targeting sequence were pLKO.1-puro-CMV-TagRFP, TRCN0000100504, and CCTGTCAGAAAGGTGACACTT, respectively. The targeting sequence targets the coding region of Arl13b starting at nucleotide 349 of the mRNA.

IMCD3 cells were transduced in a 12-well plate with the knockdown construct at a multiplicity of infection of 5. After transduction, cells were treated with puromycin at 2 μg/ml for 3 d. After treatment, cells were passaged to a six-well plate for immunofluorescence or to be harvested for Western blot analysis.

Arl13b constructs and overexpression

Arl13b was cloned using the Gateway system (Invitrogen). Full-length Arl13b (coding for amino acids 1–427 without stop codon), the N-terminal domain (coding for amino acids 1–212 of Arl13b), and the C-terminal domain (coding for amino acids 210–427 of Arl13b) were cloned into pENTR/SD/D-TOPO (K242020, Invitrogen). The inserts were recombined into the pcDNA-DEST47 (C-terminal GFP tag; 12281010, Invitrogen) and pcDNA-DEST40 (N-terminal GFP tag; 12274015, Invitrogen) using Gateway LR Clonase (11791-019, Invitrogen) following the manufacturer's instructions.

Cells (350,000 per well) were seeded in a pregelatinized six-well plate containing coverslips in DMEM (high glucose, 10% FBS, penicillin, streptomycin). After 24 h, the cells were transfected following the manufacturer's recommendations using Lipofectamine 2000 (Invitrogen) complexed with the Arl13b expression plasmids. After a 5-h incubation period of cells with the complexes, the medium was changed to serum-free DMEM High Glucose for 24 h. The cells were then fixed using 4% PFA and were subjected to immunofluorescence. Cilia were measured using LSM Image Examiner software (Carl Zeiss Microscopy, Thornwood, NY).

Arl13b-GFP expression virus

The L13 lentiviral mammalian expression vector was obtained from the Emory University Viral Vector Core. The Arl13b-GFP insert was generated by PCR from the pcDNA-DEST47 plasmid containing full-length Arl13b and using the following primers (5′ to 3′): forward-GCTAGCTCAAACAAGTTTGTACAAAAAAGC, reverse- GGATCCATTCTAGATCGAACCACTTTG. The primers introduced a 5′ *Nhe*I site and a 3′ *Bam*HI site that were used to insert Arl13b-GFP into L13.

ACKNOWLEDGMENTS

We are grateful to Kathryn Anderson, Suzie Scales, Carsten Janke, and Rajaj Rohatgi for the Smo, Gli, glutamylated tubulin (GT335), and Ptch1 antibodies, respectively. We thank Chen-Ying Su, Vanessa Horner, Alyssa Long, Miao Sun, Laura Mariani, Nicole Umberger, and Karolina Piotrowska-Nitsche for helpful comments on the manuscript. The Viral Vector Core, which generated the Arl13b-GFP lentivirus, and the Microscopy Core of the Emory Neuroscience NINDS Core Facilities were supported by National Institutes of Health (NIH) grant P30-NS055077. This work was funded by a Predoctoral Fellowship from the Greater Southeast Region American Heart Association (C.E.L.), a Basil O'Conner Starter Scholar Award from the March of Dimes (T.C.), and a research grant from the NIH (R01-NS056380).

REFERENCES

Boehlke C, Bashkurov M, Buescher A, Krick T, John AK, Nitschke R, Walz G, Kuehn EW (2010). Differential role of Rab proteins in ciliary trafficking: Rab23 regulates smoothened levels. J Cell Sci 123, 1460–1467.

Bonnafe E *et al.* (2004). The transcription factor RFX3 directs nodal cilium development and left-right asymmetry specification. Mol Cell Biol 24, 4417–4427.

Caspary T, Larkins CE, Anderson KV (2007). The graded response to Sonic Hedgehog depends on cilia architecture. Dev Cell 12, 767–778.

Cevik S, Hori Y, Kaplan OI, Kida K, Toivenon T, Foley-Fisher C, Cottell D, Katada T, Kontani K, Blacque OE (2010). Joubert syndrome Arl13b functions at ciliary membranes and stabilizes protein transport in *Caenorhabditis elegans*. J Cell Biol 188, 953–969.

Chen MH, Wilson CW, Li YJ, Law KK, Lu CS, Gacayan R, Zhang X, Hui CC, Chuang PT (2009). Cilium-independent regulation of Gli protein function by Sufu in Hedgehog signaling is evolutionarily conserved. Genes Dev 23, 1910–1928.

Corbit KC, Aanstad P, Singla V, Norman AR, Stainier DY, Reiter JF (2005). Vertebrate Smoothened functions at the primary cilium. Nature 437, 1018–1021.

Cortellino S *et al.* (2009). Defective ciliogenesis, embryonic lethality and severe impairment of the Sonic Hedgehog pathway caused by inactivation of the mouse complex A intraflagellar transport gene Ift122/Wdr10, partially overlapping with the DNA repair gene Med1/Mbd4. Dev Biol 325, 225–237.

Dave D, Wloga D, Sharma N, Gaertig J (2009). DYF-1 is required for assembly of the axoneme in *Tetrahymena thermophila*. Eukaryot Cell 8, 1397–1406.

Dishinger JF, Kee HL, Jenkins PM, Fan S, Hurd TW, Hammond JW, Truong YN, Margolis B, Martens JR, Verhey KJ (2010). Ciliary entry of the kinesin-2 motor KIF17 is regulated by importin-beta2 and RanGTP. Nat Cell Biol 12, 703–710.

D'Souza-Schorey C, Chavrier P (2006). ARF proteins: roles in membrane traffic and beyond. Nat Rev Mol Cell Biol 7, 347–358.

Eggenschwiler JT, Espinoza E, Anderson KV (2001). Rab23 is an essential negative regulator of the mouse Sonic hedgehog signalling pathway. Nature 412, 194–198.

Fan S, Fogg V, Wang Q, Chen XW, Liu CJ, Margolis B (2007). A novel Crumbs3 isoform regulates cell division and ciliogenesis via importin β interactions. J Cell Biol 178, 387–398.

Ferrante MI, Zullo A, Barra A, Bimonte S, Messaddeq N, Studer M, Dolle P, Franco B (2006). Oral-facial-digital type I protein is required for primary cilia formation and left-right axis specification. Nat Genet 38, 112–117.

Haycraft CJ, Banizs B, Aydin-Son Y, Zhang Q, Michaud EJ, Yoder BK (2005). Gli2 and Gli3 localize to cilia and require the intraflagellar transport protein polaris for processing and function. PLoS Genet 1, e53.

Houde C *et al.* (2006). Hippi is essential for node cilia assembly and Sonic hedgehog signaling. Dev Biol 300, 523–533.

Hu Q, Milenkovic L, Jin H, Scott MP, Nachury MV, Spiliotis ET, Nelson WJ (2010). A septin diffusion barrier at the base of the primary cilium maintains ciliary membrane protein distribution. Science 329, 436–439.

Huangfu D, Anderson KV (2005). Cilia and Hedgehog responsiveness in the mouse. Proc Natl Acad Sci USA 102, 11325–11330.

Huangfu D, Liu A, Rakeman AS, Murcia NS, Niswander L, Anderson KV (2003). Hedgehog signalling in the mouse requires intraflagellar transport proteins. Nature 426, 83–87.

Humke EW, Dorn KV, Milenkovic L, Scott MP, Rohatgi R (2010). The output of Hedgehog signaling is controlled by the dynamic association between Suppressor of Fused and the Gli proteins. Genes Dev 24, 670–682.
Ishikawa H, Marshall WF (2011). Ciliogenesis: building the cell's antenna. Nat Rev Mol Cell Biol 12, 222–234.
Jia J, Kolterud A, Zeng H, Hoover A, Teglund S, Toftgard R, Liu A (2009). Suppressor of Fused inhibits mammalian Hedgehog signaling in the absence of cilia. Dev Biol 330, 452–460.
Jian X, Cavenagh M, Gruschus JM, Randazzo PA, Kahn RA (2010). Modifications to the C-terminus of Arf1 alter cell functions and protein interactions. Traffic 11, 732–742.
Jin H, White SR, Shida T, Schulz S, Aguiar M, Gygi SP, Bazan JF, Nachury MV (2010). The conserved Bardet-Biedl syndrome proteins assemble a coat that traffics membrane proteins to cilia. Cell 141, 1208–1219.
Kahn RA, Cherfils J, Elias M, Lovering RC, Munro S, Schurmann A (2006). Nomenclature for the human Arf family of GTP-binding proteins: ARF, ARL, and SAR proteins. J Cell Biol 172, 645–650.
Kozminski KG, Johnson KA, Forscher P, Rosenbaum JL (1993). A motility in the eukaryotic flagellum unrelated to flagellar beating. Proc Natl Acad Sci USA 90, 5519–5523.
Li Y, Wei Q, Zhang Y, Ling K, Hu J (2010). The small GTPases ARL-13 and ARL-3 coordinate intraflagellar transport and ciliogenesis. J Cell Biol 189, 1039–1051.
Liu A, Wang B, Niswander LA (2005). Mouse intraflagellar transport proteins regulate both the activator and repressor functions of Gli transcription factors. Development 132, 3103–3111.
May SR, Ashique AM, Karlen M, Wang B, Shen Y, Zarbalis K, Reiter J, Ericson J, Peterson AS (2005). Loss of the retrograde motor for IFT disrupts localization of Smo to cilia and prevents the expression of both activator and repressor functions of Gli. Dev Biol 287, 378–389.
McMahon AP, Ingham PW, Tabin CJ (2003). Developmental roles and clinical significance of hedgehog signaling. Curr Top Dev Biol 53, 1–114.
Norman RX, Ko HW, Huang V, Eun CM, Abler LL, Zhang Z, Sun X, Eggenschwiler JT (2009). Tubby-like protein 3 (TULP3) regulates patterning in the mouse embryo through inhibition of Hedgehog signaling. Hum Mol Genet 18, 1740–1754.
Ocbina PJ, Anderson KV (2008). Intraflagellar transport, cilia, and mammalian Hedgehog signaling: analysis in mouse embryonic fibroblasts. Dev Dyn 237, 2030–2038.
Ocbina PJ, Eggenschwiler JT, Moskowitz I, Anderson KV (2011). Complex interactions between genes controlling trafficking in primary cilia. Nat Genet 43, 547–553.
Pathak N, Obara T, Mangos S, Liu Y, Drummond IA (2007). The zebrafish *fleer* gene encodes an essential regulator of cilia tubulin polyglutamylation. Mol Biol Cell 18, 4353–4364.
Patterson VL, Damrau C, Paudyal A, Reeve B, Grimes DT, Stewart ME, Williams DJ, Siggers P, Greenfield A, Murdoch JN (2009). Mouse hitchhiker mutants have spina bifida, dorso-ventral patterning defects and polydactyly: identification of Tulp3 as a novel negative regulator of the Sonic hedgehog pathway. Hum Mol Genet 18, 1719–1739.
Pedersen LB, Veland IR, Schroder JM, Christensen ST (2008). Assembly of primary cilia. Dev Dyn 237, 1993–2006.
Perdiz D, Mackeh R, Pous C, Baillet A (2010). The ins and outs of tubulin acetylation: more than just a post-translational modification? Cell Signal 23, 763–771.
Pigino G, Geimer S, Lanzavecchia S, Paccagnini E, Cantele F, Diener DR, Rosenbaum JL, Lupetti P (2009). Electron-tomographic analysis of intraflagellar transport particle trains in situ. J Cell Biol 187, 135–148.
Pugacheva EN, Jablonski SA, Hartman TR, Henske EP, Golemis EA (2007). HEF1-dependent Aurora A activation induces disassembly of the primary cilium. Cell 129, 1351–1363.
Redeker V, Levilliers N, Vinolo E, Rossier J, Jaillard D, Burnette D, Gaertig J, Bre MH (2005). Mutations of tubulin glycylation sites reveal cross-talk between the C termini of α- and β-tubulin and affect the ciliary matrix in *Tetrahymena*. J Biol Chem 280, 596–606.
Rohatgi R, Milenkovic L, Scott MP (2007). Patched1 regulates hedgehog signaling at the primary cilium. Science 317, 372–376.
Rosenbaum JL, Witman GB (2002). Intraflagellar transport. Nat Rev Mol Cell Biol 3, 813–825.
Sasaki H, Hui C, Nakafuku M, Kondoh H (1997). A binding site for Gli proteins is essential for *HNF-3*β floor plate enhancer activity in transgenics and can respond to Shh in vitro. Development 124, 1313–1322.
Taipale J, Chen JK, Cooper MK, Wang B, Mann RK, Milenkovic L, Scott MP, Beachy PA (2000). Effects of oncogenic mutations in Smoothened and Patched can be reversed by cyclopamine. Nature 406, 1005–1009.
Tran PV *et al*. (2008). THM1 negatively modulates mouse sonic hedgehog signal transduction and affects retrograde intraflagellar transport in cilia. Nat Genet 40, 403–410.
Tukachinsky H, Lopez LV, Salic A (2010). A mechanism for vertebrate Hedgehog signaling: recruitment to cilia and dissociation of SuFu-Gli protein complexes. J Cell Biol 191, 415–428.
Veland IR, Awan A, Pedersen LB, Yoder BK, Christensen ST (2009). Primary cilia and signaling pathways in mammalian development, health and disease. Nephron Physiol 111, p39–53.
Vierkotten J, Dildrop R, Peters T, Wang B, Ruther U (2007). Ftm is a novel basal body protein of cilia involved in Shh signalling. Development 134, 2569–2577.
Wang B, Fallon JF, Beachy PA (2000). Hedgehog-regulated processing of Gli3 produces an anterior/posterior repressor gradient in the developing vertebrate limb. Cell 100, 423–434.
Wen X, Lai CK, Evangelista M, Hongo JA, de Sauvage FJ, Scales SJ (2010). Kinetics of hedgehog-dependent full-length Gli3 accumulation in primary cilia and subsequent degradation. Mol Cell Biol 30, 1910–1922.
Wiens CJ *et al*. (2010). Bardet-Biedl syndrome-associated small GTPase ARL6 (BBS3) functions at or near the ciliary gate and modulates Wnt signaling. J Biol Chem 285, 16218–16230.
Zhou C, Cunningham L, Marcus AI, Li Y, Kahn RA (2006). Arl2 and Arl3 regulate different microtubule-dependent processes. Mol Biol Cell 17, 2476–2487.